Sensors and Actuators B 136 (2009) 177–185

Contents lists available at ScienceDirect

Sensors and Actuators B: Chemical

journal homepage: www.elsevier.com/locate/snb

Development of a microelectrode array sensing platform for combination electrochemical and spectrochemical aqueous ion testing

Robert D. Gardner[a], Anhong Zhou[a,*], Nephi A. Zufelt[b]

[a] Department of Biological and Irrigation Engineering, Utah State University, 4105 Old Main Hill, Logan, UT 84322-4105, USA
[b] Department of Mechanical and Aerospace Engineering, Utah State University, 4130 Old Main Hill, Logan, UT 84322-4130, USA

ARTICLE INFO

Article history:
Received 15 July 2008
Received in revised form 12 October 2008
Accepted 24 October 2008
Available online 5 November 2008

Keywords:
Microelectrode array
Potassium ferricyanide
Spectrochemical analysis
Photolithography
Electrochemical cell

ABSTRACT

A microelectrode array sensor platform was designed and fabricated to increase diversity, flexibility, and versatility of testing capabilities over that of traditionally reported sensor platforms. These new sensor platforms consist of 18 individual addressable microelectrodes, photolithography fabricated, that employ a glass base substrate and a resist polymer layer that acts as an insulating agent to protect the circuitry and wiring of the sensor from undesired solution interactions. Individually addressable microelectrodes increase diversity by allowing isolated electrochemical testing between electrodes, global array testing, or some combination of electrodes to perform electrochemical methods. Furthermore, because of the optical transparency of the glass base substrate and the resist mask layer, along with the small size of the electrode array, spectrochemical analysis is possible within the sample area that acts as electrochemical cell and cuvette, while the microelectrode array passively resides within the optical path length during spectrochemical testing. This unique arrangement offers improved testing possibilities for various applications, including simultaneous electrochemical and spectrochemical analysis in environmental testing, identification or quantification of possible species for bioavailability in the biotechnology field, and process control in industrial applications. Electrochemical characteristics and spectrochemcial use of the sensor platform are proven with potassium ferricyanide, an electrochemical standard analyte, and electrochemical measurements are compared against a commercially available working electrode of similar size. Additionally, the electrochemical method of differential pulse anodic stripping voltammetry is performed with the sensor platform to detect copper and lead heavy metal ions in aqueous solution, demonstrating the potential for use with environmental samples.

1. Introduction

Trace chemical species identification and quantification are critical to analytical chemistry experiments in industrial, environmental, and academic research. Many systems and environments require testing for trace levels of ions or molecules that reside, contaminate, or transform through some reaction. Salinity is an important criterion of water control in both agricultural and municipal water supplies. Salts are strong electrolytes consisting of metal cations and counter ions that disassociate in aqueous solutions. Metal contaminates such as copper, lead, zinc, and cadmium can be present in foods, beverages, drinking water, and aquatic environments [1–4]. Alternatively, ions can be important trace nutrients for biological species growth in an aqueous medium, and monitoring their concentrations can improve the information derived from laboratory studies. Because charged species have the potential to improve studies or raise levels of concern, accurately monitoring or quantifying them is of great importance.

Traditionally, environmental or industrial process samples are collected on site and removed to a laboratory facility where electrochemical, chromatographic, and spectroscopic methods are employed to detect, observe, and quantify ions or ionic species within the sample. Examples of typical methods utilized include: inductively coupled plasma-mass spectrometry (ICP-MS), differential pulse anodic stripping voltammetry (DPASV) on mercury based electrodes, graphite furnace atomic absorption spectrometry (GF-AAS), cold vapor atomic absorption spectrometry (CV-AAS), and cold vapor atomic fluorescence spectrometry (CV-AFS) [5–7]. While many of these methods capitalize on low detection abilities and large linear dynamic concentration test ranges, these test methods can be insensitive to some of the charged species of interest and take an undesirably long amount of time to report results. The samples also have a greater chance of exposure to contamination due to the transportation and relocation prior to testing [1,8].

* Corresponding author. Tel.: +1 435 797 2863; fax: +1 435 797 1248.
E-mail address: Anhong.Zhou@usu.edu (A. Zhou).

0925-4005/$ – see front matter © 2008 Elsevier B.V. All rights reserved.
doi:10.1016/j.snb.2008.10.031

Some advantages of new analytical tools and sensors that are capable of real-time process monitoring or environmental monitoring include: improved process control, minimization of environmental impact, and continuous monitoring capabilities with options for early detection [1,2]. By offering rapid return of results, early action can be initiated when problematic issues are detected within systems.

Ions and charged species of interest can be monitored on site with an appropriately designed sensor with the aforementioned capabilities. Additionally, with the advances and trends toward cleaner (green) analytical chemistry, a new sensor system should be capable of monitoring an environment without polluting the system or affecting it in any adverse manner [1]. Electrochemical (EC) methods have been proven effective for ion detection. Features like independence from an optical path length and high sensitivity approaching that of fluorescence, along with low power requirements, low cost, ability to be miniaturized, and adaptability with advanced micromachining and microfabrication technologies, all increase the appeal of this test method [1]. Furthermore, by appropriate design of the sensor platform, the EC system can reside in a quasi-passive manner, allowing traditional spectrochemical (SC) methods to be employed. New analytical tools that offer greater diversity and flexibility in testing increase application versatility.

Traditionally, EC working electrodes are large electrodes in the centimeter or millimeter scale. However, since the advent of microelectrodes, it is no longer necessary to rely on bulky electrodes or difficult electrochemical cells when fast, easy, environmentally friendly electrochemical systems can be designed [1]. Additionally, miniaturization of electrodes offers many practical and fundamental advantages: reduced resistance (ohmic drop), reduced sample consumption, ability to incorporate many electrodes in a small area, and increased ability to facilitate measurements in low-ionic-strength water samples [1].

The foremost advantage of using this miniaturized electrode is the mass transport enhancement due to nonlinear diffusion properties, which is further amplified when multiple electrodes are utilized in an array. Nonlinear diffusion occurs at the boundary of the electrode due to the increased perimeter-to-surface area exhibited by microelectrodes, as compared to larger traditional electrodes. Current density is increased at the electrode boundaries, yielding current amplification [3,9–15]. Extensive work has been done to show that microdisk designs (circular shaped disk) have hemispherical diffusion patterns and microband designs have hemispherical or a combination of hemicylindrical-hemispherical diffusion patterns depending on whether they are square- or rectangular-shaped, respectively [3,9,13,15]. Furthermore, 3-D (hemispherical) diffusion associated with microelectrodes has a steady state analyte mass flux to the electrode surface, resulting in sigmoidal cyclic voltammograms instead of the peak shaped voltammograms observed with traditional or non-square microband electrodes [3,15]. With their small size, larger perimeter-to-surface area, and nonlinear radial diffusion through the diffusion zones, microelectrodes attain larger response changes and improved signal-to-noise ratios.

By utilizing microelectrodes in an array fashion, one can capitalize on the enhanced properties inherent in the smaller microelectrode size. Additionally, a greater diversity of testing is possible with a sensor platform capable of multiple microelectrode combinations. With the use of a multi-channel potentiostat or a multiplexer, one can simply use all microelectrodes independently, cycling through each electrode, scanning at different potential ranges; or use the microelectrodes as a census electrode with all electrodes performing as one to capitalize on their individual enhancements while allowing greater current flow. This is beneficial due to the small current (nA–pA) associated with individual microelectrodes. The option also exists for some situationally unique combinations of the two former scenarios. In these cases, inter-electrode spacing must be such that diffusion zones from the individual microelectrodes do not overlap to constructively interfere and produce planar diffusion zones like those associated with macroelectrodes. Extensive studies comparing inter-electrode spacing with current responses have reportedly used or suggested using an inter-electrode spacing of 10 times the width, or diameter, of the electrode [2,3,15–17].

As previously mentioned, spectroscopy within the sensor test area can be realized with intelligent design in the base sensor substrates and a complimentary insulation mask layer to isolate circuitry. In the majority of cases, microelectrodes are grown, deposited, or printed on silicon or silicon carbide base materials; however, glass or polished quartz offer the benefits of low electrical conductivity and optical transparency. Also, there are a variety of mask layers that can be utilized in this type of sensor platform including oxide, silicon nitride, or simple resist coatings [10,14,17]. Based on the 1981 work by Aoki, as well as fabrication simplicity, the resist polymer coating was deemed advantageous over other coatings, although silicon nitride would be less susceptible to corrosion [10,17]. Furthermore, thin resist layers maintain transparency characteristics which allow spectroscopic measurements to be made, while silicon nitride would not. By using the simplistic fabrication approach of opening holes in the resist mask layer directly above the electrodes and then utilizing plasma etch to clean the electrode surface, low cost, reliable, and sensitive sensor platforms can be developed. This approach has been performed on a traditional macroelectrode and with silicon based platforms, but a literature search failed to show where it has been performed on a microelectrode array for use in both EC and SC testing [10,14]. Additionally, the transient current response through recessed microelectrodes maintains the current amplification from the enhanced nonlinear diffusion [9].

This paper is a summary of the work done to develop a low cost, reliable sensor platform that is sensitive and selective to ions that may act as interesting constituents or contaminates in aqueous systems. This platform utilizes miniaturized microelectrodes that reside in a planar array design for use in EC test methods that, when coupled with working microelectrodes, allow trace levels of ions to be detected. Additionally, due to the small size of the microelectrode array (MEA), SC methods may be employed on analyte aqueous solutions where the sample container acts as both cuvette and EC cell for SC and EC techniques, respectively. SC methods can add diversity in testing, allowing additional information to be obtained in aqueous systems. This work has demonstrated the capability to simultaneously conduct EC and SC measurements of metal ions in an aqueous sample, which provides new opportunities to develop a portable, environmentally friendly, and reliable sensing systems for water quality monitoring.

2. Experimental

2.1. Microelectrode sensor design

The MEAs are based on a planar design where 10 μm × 10 μm gold working electrodes are positioned (1 μm thick) on glass to form arrays. Adequate adherence to glass is accomplished by a thin (50 nm) layer of titanium between the gold surface and glass support base. Glass was chosen as the support base for its low electrical conductivity and optical transparency. The exact geometry of these electrodes and arrays is as follows: nine 50 μm × 50 μm base electrode pads with 30 μm circuitry connecting the electrode with outer slide edge electronic connection pads, utilized for connection

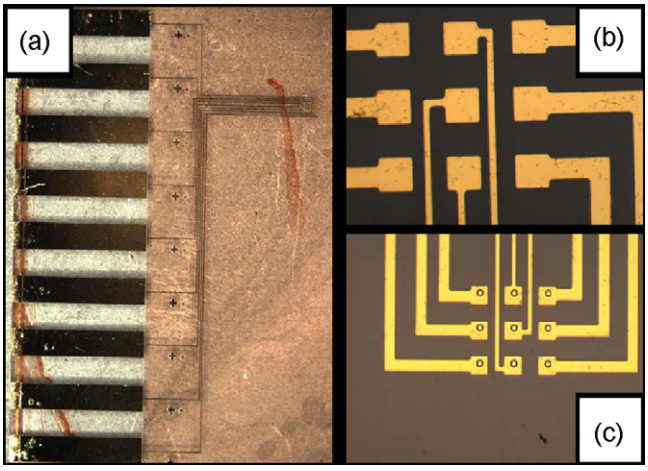

Fig. 1. Half array pictures: (a) final half array comprising of nine electrodes, wiring, and electronic contact pads; magnified views of the nine electrode test site (b) before and (c) after the final layer of resist is applied and electrode holes are opened.

to an external electrochemical analyzer, comprise half an array. Two half arrays work together to form an array with connection pads on each side of the glass slide. The three central electrodes in a nine electrode half array have short spans of 10 μm circuitry for ease in fabrication. A final layer of Shipley photoresist 1813 masks the entire slide with the exception of the 10 μm × 10 μm holes positioned over the 50 μm × 50 μm pads and the electronic connection pads on the glass slide edge. Fig. 1 shows these half arrays both before and after the final photoresist mask is applied and heat treated. Fig. 2 shows a finished glass slide for electrochemical configuration, with all the individual electrodes comprising the three arrays, as well as the numbering scheme developed to label each microelectrode. Sensor platform attachment to a 96-welled plate for spectroscopic measurements is not shown.

2.2. Photolithography fabrication of MEAs

Sensors were constructed by implementing basic photolithography methodology utilized in integrated circuit fabrication. Electron beam sputtering was employed to deposit a thin layer of titanium, approximately 50 nm, to the exterior of a glass microscope slide acting as bonding agent between glass elements and a gold layer, approximately 1 μm thick. Layer thicknesses were monitored with a piezoelectric quartz crystal microbalance thickness monitor. Gold-coated slides were stripped to exact geometries specified for the 54 individually isolated electrodes with a photolithography technique, summarized as follows:

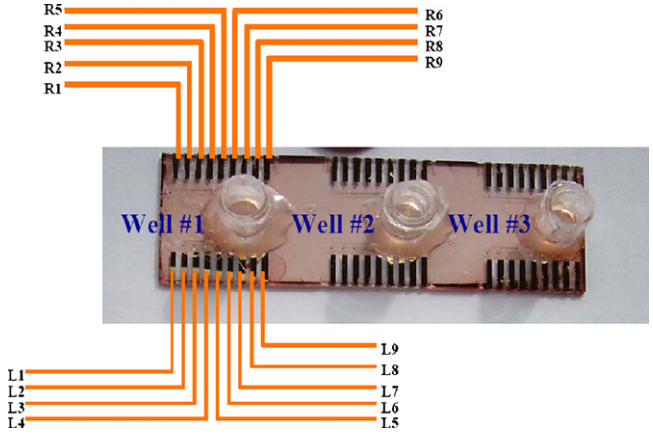

Fig. 2. Complete microelectrode array platform and numbering designation for electrochemical experimentation configuration.

A. Shipley photoresist 1813 was applied to thickness by spinning 40 s at 2000 rpm on a spin coater. The photoresist was soft heat set on the slide surface by heating to 95 °C for 90 s on a general hot plate.
B. The slide was then exposed, on a mask aligner, to light from a mercury lamp at 365 nm wavelength for 8 s, followed by development and deionized water rinse.
C. The gold layer was removed from everywhere exposed to UV light with an iodine based gold etch, followed by a buffered oxide etch (BOE) to remove the titanium layer. The remaining metal comprised the contact pads, circuitry, and electrode pads on the slides.
D. A second layer of Shipley photoresist 1813 was spun and heat set at the parameters previously reported, followed by UV exposure in a mask aligner with a secondary mask exposing 10 μm × 10 μm holes over each 50 μm × 50 μm electrode pad as well as the electronic contact pads on outer slide edge. Once more, development and rinsing were preformed with the previous parameters.
E. Electrode surfaces were cleaned with an evacuated oxygen plasma etch for 1 min to remove organic material.

The slides were completed with three arrays per slide, giving a total of 54 individually isolated working electrodes per slide. The final step in sensor construction was the adhesion of sterol plastic wells cut from a 96-well plate, or attachment, to the bottom of a 96-well plate for spectroscopic testing. This prototype sensor platform was designed for future application and coupling with a 96-well plate; herein we report experimental results from wells previously cut out of the plate and adhered to the sensor for EC testing, and platforms attached to the 96-well plate for SC testing. The attachment was accomplished using a non-conductive, solvent free, urethane epoxy (Royal-Hardman), shown to have no effect on the photoresist mask or the individual circuitry that comprised the MEA.

2.3. Electrochemical measurements and reagents

All electrochemical testing was performed using a CHI 1220 Electrochemical Analyzer (CH Instruments, TX, USA), and all experiments were done in the standard three electrode configuration. The gold electrodes of the MEA, fabricated as aforementioned, or a 10 μm gold wire working electrode (CH Instruments) were utilized

Table 1
Experimental parameters for cyclic and differential pulse anodic stripping voltammetry testing.

Parameter type	CV parameter	DPASV parameter
Initial E (V)	0.5	−0.6 (Cu & Pb)
High E (V)	0.5	0.4 (Cu & Pb)
Low E (V)	−0.1	
Input positive/negative	N	
Scan rate (V/s)	0.01	
Segment (#)	2	
Sample interval (V)	0.001	
Quiet time (s)	2	60
Sensitivity (A/V)	1×10^{-9}	1×10^{-9}
Increment E (V)		0.004
Amplitude (V)		0.025
Pulse width (s)		0.05
Sample width (s)		0.0167
Pulse period (s)		0.02

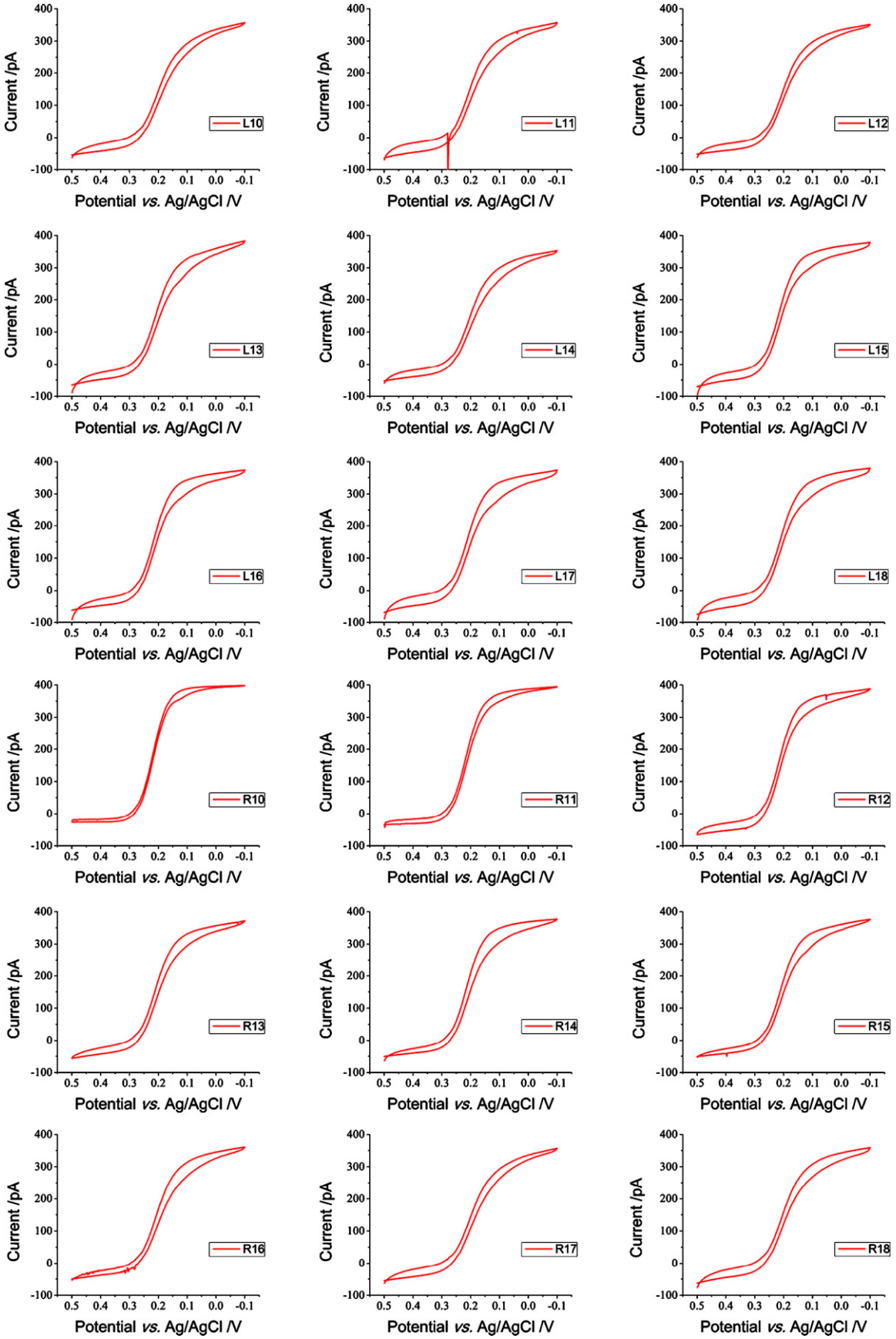

Fig. 3. Cyclic voltammograms for individual 18 MEA electrodes comprising one test site with 0.3 mM $K_3Fe(CN)_6$ in 0.01 M PBS; 0.5 to −0.1 V, scan rate of 10 mV/s.

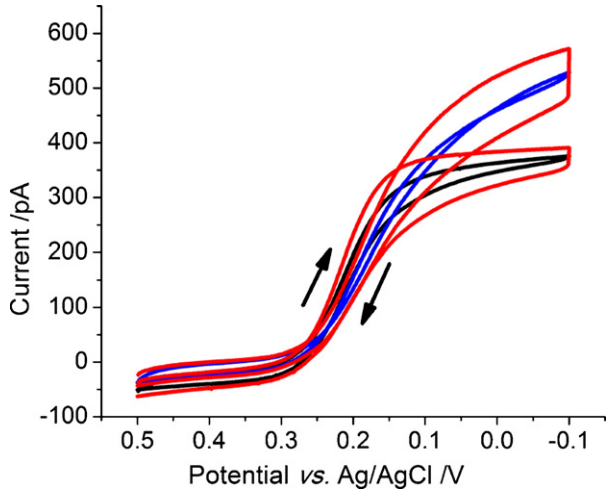

Fig. 4. Average cyclic voltammetry and standard deviation comparison for MEA electrodes comprising one test site with 0.3 mM (black sigmoidal curve set) and 0.5 mM (blue sigmoidal curve set) $K_3Fe(CN)_6$ in 0.01 M PBS, 0.5 to −0.1 V, scan rate of 10 mV/s. $n = 18$.

as the working electrode, with a silver|silver chloride (Ag|AgCl) reference electrode and platinum wire counter electrode (both from CH Instruments). Polishing of the 10 μm gold wire working electrode was done by successive polishing using 1 (bare borundum sanding paper only), 0.3, 0.1, and 0.05 μm alumina slurries, followed by thoroughly rinsing with deionized water. The MEA gold working electrodes were utilized 'as is' after the oxygen plasma etch treatment described earlier.

Cyclic voltammetry testing was performed on concentrations of 0.05, 0.1, 0.3, 0.5, 0.8, and 1 mM $K_3Fe(CN)_6$ in 0.01 M PBS (both from Sigma–Aldrich) and recorded at the working electrode. Differential pulse anodic stripping voltammetry was performed on a 50 ppb Cu and 50 ppb Pb mixed analyte solution with HNO_3 as counter electrolyte prepared from 1000 ppm, 2% HNO_3, Cu and Pb standards (Fisher Scientific) and recorded at the working electrode. This solution was diluted to exact concentration with 18 MΩ deionized water. The $K_3Fe(CN)_6$ in 0.01 M PBS solutions and 50 ppb Cu and Pb in deionized H_2O were deoxygenated by nitrogen purge for at least 10 min prior to testing. Table 1 shows the experimental parameters for cyclic and differential pulse anodic stripping voltammetry testing.

The electrochemical cell consisted of a sterol plastic well approximately 300 μl volume (cut from a Falcon flat bottom 96-well plate) for the MEA working electrode tests, and a 25 ml glass beaker, for the 10 μm gold wire working electrode tests. The counter and reference electrodes were inserted through the top opening for the MEA working electrode tests, and all three electrodes were inserted through the top opening of the glass beaker for the 10 μm Au wire working electrode tests.

Spectrochemical analysis was performed using Multiskan Spectrophotometer (Thermo Labsystems, MA, USA) in 96-well plate configuration utilizing 0.01 M PBS and 1.0 mM $K_3Fe(CN)_6$ in a 0.01 M PBS solution. The MEA sensor platform was attached to the bottom of a modified Falcon flat bottom 96-well plate.

3. Results and discussion

Initial tests to investigate electrochemical behaviors and to determine if the MEA electrodes are operational were performed using cyclic voltammetry (CV) measurements on the ferric/ferrocyanide redox couple. It is essential to verify the operation of each electrode in an array format before more advanced EC testing methods may be employed utilizing these electrodes. Solutions of 0.3 and 0.5 mM $K_3Fe(CN)_6$ in 0.01 M PBS were tested on all 18 individual MEA electrodes within one test site, utilizing the potential range 0.5 to −0.1 V and a scan rate of 10 mV/s. Fig. 3 shows the individual plots for the 18 electrodes comprising one test site on the sensor platform. Each individual MEA electrode portrays the steady state sigmoidal shape with no transient limited peak indicative of nonlinear diffusion and current density enhancement. Furthermore, the responses are in agreement with CV curves from literature [3,14,17,18]. The individual plots for the 18 electrodes tested at 0.5 mM $K_3Fe(CN)_6$ in 0.01 M PBS were not included in this report but are similar in form to those shown in Fig. 3.

The average response, with standard deviation, between the 18 electrodes at both 0.3 and 0.5 mM $K_3Fe(CN)_6$ in 0.01 M PBS is shown in Fig. 4. There is a small amount of variation between electrodes at both 0.3 mM and 0.5 mM $K_3Fe(CN)_6$ in 0.01 M PBS. The responses indicate a lower amount of variation at the lower 0.3 mM concentration than that of the higher 0.5 mM concentration. A possible reason for the variance may be saturation of the sensor's ability to reduce

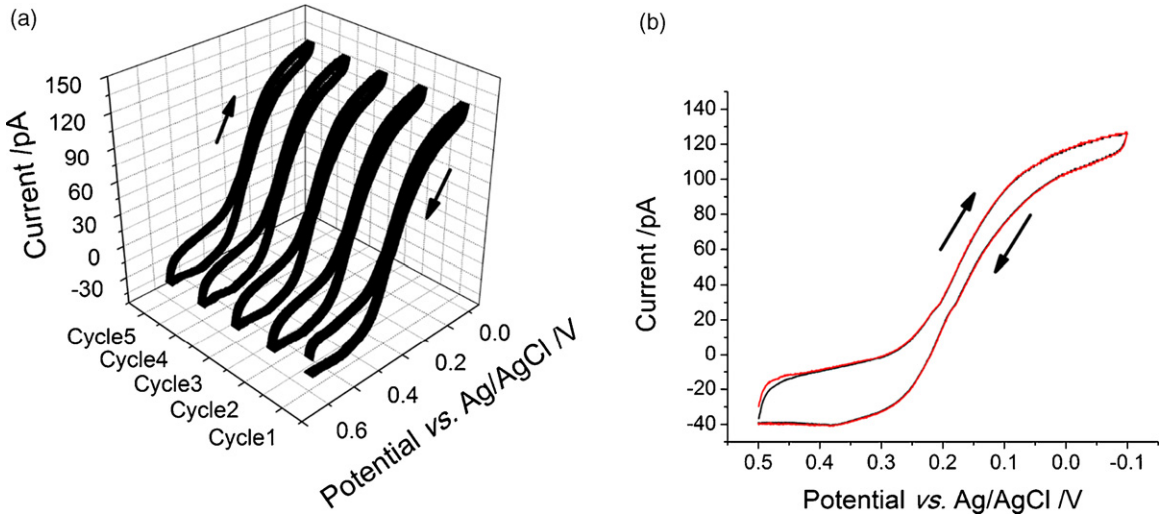

Fig. 5. Cyclic voltammetry testing of a microelectrode array electrode in (a) five successive tests and (b) average and standard deviation with 0.1 mM $K_3Fe(CN)_6$ in 0.01 M PBS, 0.5 to −0.1 V with scan rate of 60 mV/s. Arrow indicates the potential scanning direction. $n = 5$.

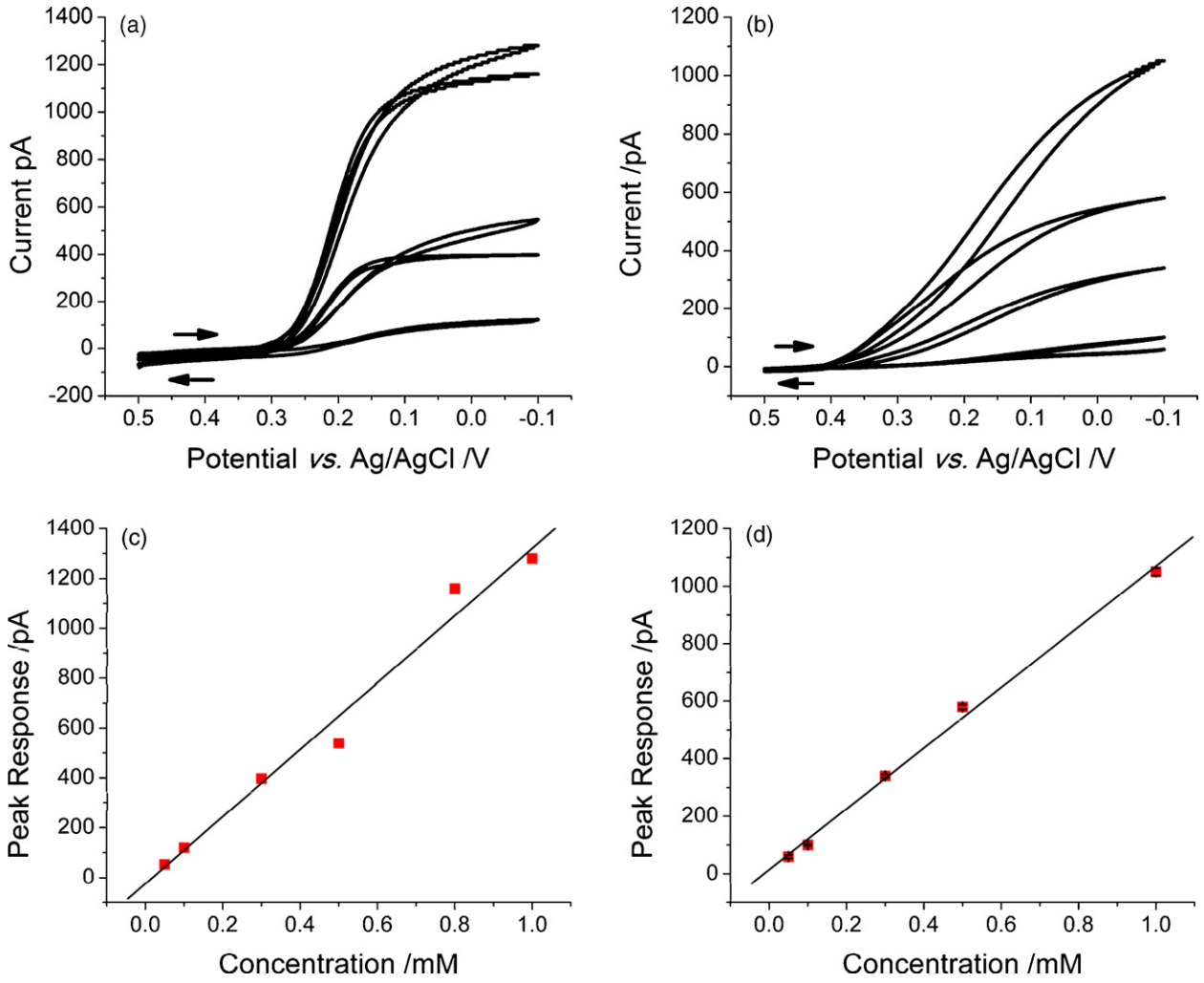

Fig. 6. Cyclic voltammetry of $K_3Fe(CN)_6$ using (a) microelectrode array electrode and (b) 10 μm CH electrode at concentrations of 0.05 (lower curve), 0.1, 0.3, 0.5, 0.8, and 1 mM (upper curve) in 0.01 M PBS supporting electrolyte, 0.5 to −0.1 V with scan rate in all cases of 10 mV/s. Arrow indicates the potential scanning direction. Plots of peak currents vs. mediator concentration and linear fits (solid lines) for (c) microelectrode array electrode and (d) 10 μm CH electrode.

and oxidize the $K_3Fe(CN)_6$ by excess analyte in solution, indicating that the linear full span output or the linear testing range of the sensor has been surpassed and the response has become nonlinear as it approaches some asymptotic current value. Another possible reason for the small variation is in the small circuitry resistive differences between the electrodes comprising an array. At this point, we believe the variation increase in 0.5 mM compared to that of 0.3 mM to be a product of resistance difference between individual microelectrodes.

In spite of the small variation between electrodes, there is significant difference between responses at the tested concentrations. As expected, the higher 0.5 mM analyte concentration gave a response of approximately 530 pA, compared to approximately 360 pA for the 0.3 mM analyte, as shown in Fig. 4. Furthermore, the average responses of the 18 MEA electrodes, with respect to both concentrations, have non-overlapping standard deviation differences.

Repeatability and drift characteristics were investigated by five successive runs with 0.1 mM $K_3Fe(CN)_6$ in 0.01 M PBS, 0.5 to −0.1 V with scan rate of 60 mV/s, shown in Fig. 5; (a) shows individual five cycle voltammograms and (b) shows the average between the cycles and standard deviation between cycles. Again the sigmoidal steady state curve is present with no transient diffusion limited peaks indicative of the current density and diffusional enhancements. Results indicate these electrodes have a high degree of repeatability as no significant drift is observed over the five runs tested. There was a slight difference with the initial onset of the reducing path observed on the first cycle tested, but it is negligible because the maximum current response is correlated with concentration, which lies at the end of the reducing path at −0.1 V. At this maximum current response, there is almost no difference between the five cycles tested, as noted by the standard deviation residing atop the average, shown in red and black, respectively, in Fig. 5.

Fig. 6 shows CV testing from .5 to −0.1 V with a scan rate of 10 mV/s on solutions of (a) 0.05, 0.1, 0.3, 0.5, 0.8, and 1 mM $K_3Fe(CN)_6$ in 0.01 M PBS for a MEA electrode, and (b) 0.05, 0.1, 0.3, 0.5, and 1 mM $K_3Fe(CN)_6$ in 0.01 M PBS for a 10 μm electrode purchased from CH Instruments for comparison reasons. The sigmoidal shape curve is observed on all the responses within the concentration range tested with no transient limited peak formation, for the MEA electrode. The sigmoidal steady state shape curve is present with concentrations greater than and equal to 0.3 mM for the 10 μm CH electrode; however, the low concentrations 0.05 and 0.1 mM did not have a sigmoidal shape, but rather increased to a maximum current response at −0.1 V. At 0.5 V, the response returned to the initial state, but did not come to a resolving plateau. This indicates the solution was continuously reduced and oxidized throughout the entire reducing and oxidizing passes, respectively. In other words, there is implication that the full extent of combined

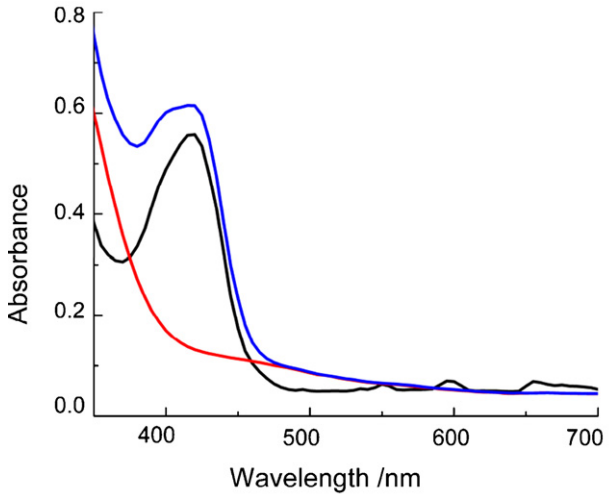

Fig. 7. Absorbance in the visible spectrum of (red) 0.01 M PBS and (blue) 1 mM $K_3Fe(CN)_6$ in 0.01 M PBS when a microelectrode array with resist polymer coating is attached to the bottom of a 96-well plate. A control (black) of 1 mM $K_3Fe(CN)_6$ in 0.01 M PBS in an unaltered well is shown for comparison. 350–700 nm with a scan increment of 5 nm.

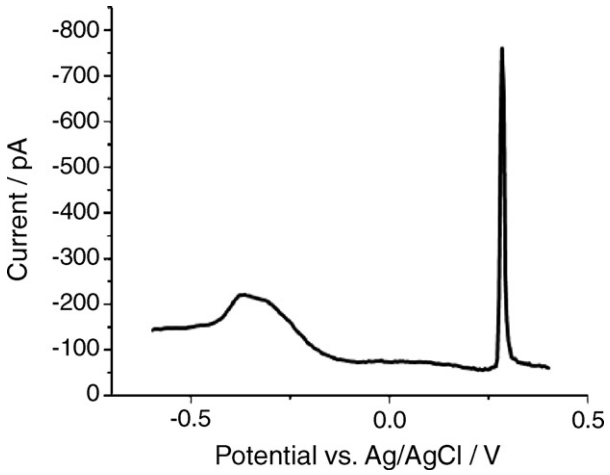

Fig. 8. Microelectrode array electrode L8 differential anodic stripping voltammetry testing on 50 ppb Cu and 50 ppb Pb in HNO_3 solution, 60 s preconcentration, −0.6 to 0.4 V scan range.

linear and nonlinear diffusion was not achieved by this commercial 10 μm electrode when tested in these low analyte concentrations.

Peak current response vs. mediator concentration plots were constructed for (c) MEA CV results and (d) 10 μm CH electrode CV results. There is a strong linear correlation to the concentration responses for both electrodes tested, where the squared correlation coefficient (R^2) equals 0.981 and 0.991, for the MEA electrode and the 10 μm CH electrode, respectively. The span output over the concentrations tested occurred with the highest concentration tested (1.0 mM) and is approximately 1.3 and 1.1 nA for the MEA electrode and the 10 μm CH electrode, respectively. This indicates the MEA electrode is more sensitive to the same concentration of $K_3Fe(CN)_6$ within the solution ranges tested.

In order to test the MEA sensor platform's ability to act passively when spectrochemical tests occur within the electrochemical cell acting as cuvette, a MEA sensor slide was attached to the bottom of a Falcon 96-well spectrophotometric plate. The excitation light passed from the top of the well, through the analyte solution, then through the MEA sensor slide to the photomultiplier tube. Fig. 7 shows the visible absorbance spectrum of 0.01 M PBS, shown in red, and 1 mM $K_3Fe(CN)_6$ in 0.01 M PBS, shown in blue, where the microelectrode array (resist polymer coating included) is attached to the bottom of the well. Also included is a control measurement of 1 mM $K_3Fe(CN)_6$ in 0.01 M PBS, shown in black, measured within an unaltered well. Absorbance was measured from 350–700 nm with a scan increment of 5 nm. Comparison between the 1 mM $K_3Fe(CN)_6$ in 0.01 M PBS and 0.01 M PBS responses show a distinct absorbance peak at approximately 410 nm attributed to the $K_3Fe(CN)_6$ analyte. The wavelength is confirmed by comparison with 1 mM $K_3Fe(CN)_6$ in 0.01 M PBS tested in an unaltered well, where the same peak formation was observed. There was an increase in absorbance at 410 nm between the MEA altered and native curves, blue and black, respectively. This increase in sensitivity can be attributed to possible advantageous optical transparency characteristics of the glass based MEA sensor substrate as opposed to the native characteristics of the unaltered plastic 96-well plate holds, or a linear combination of increased absorbance the MEA slide may impose at 410 nm. However, the significant absorbance signal recorded in the presence of the MEA sensor platform confirms the ability to passively reside within the optical path length during spectrochemical analysis, thus adding a new dimension to the testing ability of the MEA sensor platform when attached to a 96-well plate.

Although the EC and SC results and discussion have thus far been conducted independently, the very positive results for both types of testing methods drive future research toward simultaneous SC and EC testing. Thus, the combined sensor platform offers many possibilities, in many fields, to increase the speed and diversity of testing. For instance, environmental water samples can be taken for both optical density measurements and heavy metal ion analysis. This sensor platform will allow simultaneous testing for the desired investigations. Toward that end, a MEA electrode was utilized to perform stripping analysis with differential pulse anodic stripping voltammetry (DPASV) in order to demonstrate the EC component of the platform for such an investigation.

Stripping analysis is a powerful electrochemical technique capable of detecting metals at trace concentrations [1–4,6,8,11,18–21]. DPASV is essentially a two phase testing technique. Phase one employs an underpotential held constant for a certain amount of time, effectively reducing and electroplating the electrochemical analyte on the electrode surface. Phase two begins sweeping the potential towards overpotential and the plated analyte is oxidized and stripped off. Electrochemical analytes (e.g., heavy metal ions) have different oxidation–reduction potentials specific to the analyte species of interest, and stripping the analyte from the electrode surface causes a significant change in current at this oxidation–reduction potential. Therefore, this testing technique can be utilized on individual or mixed analyte systems where analyte concentrations are correlated to the change in current registered at oxidation–reduction potentials which will show as peaks on voltammograms recorded during the sweeping phase of DPASV testing. Speciation is accomplished by correlating oxidation potentials of analytes to peaks of the voltammogram.

DPASV was done on 50 ppb mixed Cu and 50 ppb Pb solutions with HNO_3 as the counter electrolyte. Fig. 8 shows the DPASV responses of the 50 ppb analyte solutions, with scanning range of −0.6 to 0.4 V, 60 s quiescent preconcentration. Both Pb and Cu attributed peaks are present at the expected ranges, −0.4 to −0.25 V and 0.2 to 0.35 V, respectively. These peak potential positions coincide with published literature reports [3,18,19]. This indicates that our design for microelectrodes can successfully detect individual current changes associated with each analyte. The Cu peak is narrow with respect to the Pb peak, and this peak narrowing could be due to differences in preconcentration effects on the stripping

response, diffusion rate differences between Cu and Pb, or non-uniform electroplating of the Cu ions to the electrode surface. Further investigation into counter electrolyte concentration effect and preconcentration parameters may shed light on the narrow peak effect. However, for the purpose of proving the sensor platform for application in heavy metal ion detection by stripping analysis, these results indicate an excellent ability for heavy metal ion detection.

The use of a multi-channel potentiostat or multiplexer interfacing with our MEA sensors simplifies these measurement procedures: (1) conducting different electrochemical measurements in each single microelectrode. For example, one microelectrode can run cyclic voltammetry, and the other one can run ASV or DPASV, (2) any selected microelectrodes can be conductively connected by simply modifying the lithography procedures. This configuration would result in higher current responses compared to the single microelectrode.

Fig. 8 demonstrates the ability of our MEA sensor to detect multiple heavy metal ions, which is important in water quality monitoring and management. The application of this sensor platform to real water samples and the re-configuration of MEA patterns to increase sensor sensitivity are under investigation.

4. Conclusion

A microelectrode array sensor platform was designed and fabricated, by lithographic means, to effectively increase diversity and versatility of testing capabilities over that of traditionally reported macroelectrode sensors. These MEA sensor platforms consist of 18 individually addressable microelectrodes and employ a resist layer as an insulating layer protecting the circuitry and wiring of the sensor. The microelectrodes were defined by holes opened in the resist mask layer to exact electrode dimensions. Furthermore, these MEA sensor platforms consist of planar arrays of gold square microelectrodes with an interelectrode spacing of 100 μm, making the interelectrode spacing 10× the width (10 μm × 10 μm square) of the electrode, effectively enhancing the mass transport properties of the electrochemical analyte by allowing nonlinear diffusion around the perimeter of the electrode.

The enhancement of mass transport was checked by cyclic voltammetry on the ferric/ferrocyanide redox couple, and exhibited well defined sigmoidal shaped curves which signify 3-D hemispherical diffusion of the electrochemical analytes. Drift was checked by repeating the cyclic voltammetry testing five times; observations indicated high repeatability. The MEA sensor was compared against a commercially available 10 μm CH electrode in cyclic voltammetry testing. Evidence suggests that the MEA electrodes perform better than the 10 μm CH electrode in both increased sensitivity and better theoretically defined voltammograms.

Additionally, these investigations have demonstrated that, when a glass base substrate with a relatively optically transparent resist mask layer is utilized, spectrochemical analysis is possible within the sample area that would act as the electrochemical cell and cuvette. This capability increases the diversity and versatility of the testing that can be performed with this sensor platform. The ability of the sensor platform to detect Cu and Pb heavy metal ions in aqueous solutions was also proven by utilizing the electrochemical method of differential pulse anodic stripping voltammetry.

Acknowledgement

We appreciate the financial support from the Utah Water Research Laboratory, Logan, UT, and from USU New Faculty Start-up funds (A.Z.). We are also thankful to the Undergraduate Research and Creative Opportunities (URCO) program supported by USU Vice President for Research Office (R.G. and N.Z.). R.G. is also partially supported by NIH (#ES013688-01A1) (A.Z.) and USU College of Engineering Dean's Teaching Funds. Special thanks are reserved for Dr. Brian Baker from the MicroFab Lab at the University of Utah for help with sensor fabrication procedures.

References

[1] J. Wang, Real-time electrochemical monitoring: toward green analytical chemistry, Accounts of Chemical Research 35 (2002) 811–816.
[2] R. Feeney, S.P. Kounaves, Microfabricated ultramicroelectrode arrays: developments, advances, and applications in environmental analysis, Electroanalysis 12 (2000) 677–684.
[3] A. Berduque, Y.H. Lanyon, V. Beni, G.e. Herzog, Y.E. Watson, K. Rodgers, F. Stam, J. Alderman, D.W.M. Arrigan, Voltammetric characterisation of silicon-based microelectrode arrays and their application to mercury-free stripping voltammetry of copper ions, Talanta 71 (2007) 1022–1030.
[4] J. Wang, Stripping Analysis: Principles, Instrumentation, and Applications, VCH Publishers, INC, Deerfield Beach, Florida, 1985.
[5] R. Piech, W.W. Kubiak, Determination of trace arsenic with DDTC-Na by cathodic stripping voltammetry in presence of copper ions, Journal of Electroanalytical Chemistry 599 (2007) 59–64.
[6] A. Giacomino, O. Abollino, M. Malandrino, E. Mentasti, Parameters affecting the determination of mercury by anodic stripping voltammetry using a gold electrode, Talanta 75 (2008) 266–273.
[7] Annual Book of ASTM Standards, Section 11, Water and Environmental Technology.
[8] G. Forsberg, J.W. O'Laughlin, R.G. Megargle, S.R. Koirtyohann, Determination of arsenic by anodic stripping voltammetry and differential pulse anodic stripping voltammetry, Analytical Chemistry 47 (1975) 1586–1592.
[9] J.A. Alden, J. Booth, R.G. Compton, R.A.W. Dryfe, G.H.W. Sanders, Journal of Electroanalytical Chemistry 389 (1995) 45–54.
[10] K. Aoki, J. Osteryoung, Diffusion controlled current at a stationary finite disk electrode, Journal of Electroanalytical Chemistry 125 (1981) 315–320.
[11] A.S. Baranski, H. Quon, Potentiometric stripping determination of heavy metals with carbon fiber and gold microelectrodes, Analytical Chemistry 58 (1986) 407–412.
[12] D.K. Cope, D.E. Tallman, Transient behavior at planar microelectrodes: A comparison of diffusion current at ring, band and disk electrodes, Journal of Electroanalytical Chemistry 285 (1990) 85–92.
[13] P.M. Kovach, W.L. Caudill, D.G. Peters, R.M. Wightman, Faradaic electrochemistry at microcylinder, band, and tubular band electrodes, Journal of Electroanalytical Chemistry 185 (1985) 285–295.
[14] W. Thormann, P.v.d. Bosch, A.M. Bond, Voltammetry at linear gold and platinum microelectrode arrays produced by lithographic techniques, Analytical Chemistry 57 (1985) 2764–2770.
[15] M. Wittkampf, K. Cammann, M. Amrein, R. Reichelt, Characterization of microelectrode arrays by means of electrochemical and surface analysis methods, Sensors and Actuators B Chemical 40 (1997) 79–84.
[16] L.A. Dunyushkina, Y. Lu, S.B. Adler, Microelectrode array for isolation of electrode polarization on planar solid electrolytes, Journal of the Electrochemical Society 152 (2005) A1668–A1676.
[17] M. Kudera, H.A.O. Hill, P.J. Dobson, P.A. Leigh, W.S. McIntire, Electrochemical characterisation and application of multi microelectrode array devices to biological electrochemistry, Sensors 1 (2001) 18–28.
[18] S.B. Saban, R.B. Darling, Multi-element heavy metal ion sensors for aqueous solutions, Sensors and Actuators B Chemical 61 (1999) 128–137.
[19] R.A.A. Munoz, P.V. Oliveira, L.U. Angnes, Combination of ultrasonic extraction and stripping analysis: an effective and reliable way for the determination of Cu and Pb in lubricating oils, Talanta 68 (2006) 850–856.
[20] C.F. Pereira, F.B. Gonzaga, A.M. Guaritïa-Santos, J.R. SouzaDe, Determination of Se(IV) by anodic stripping voltammetry using gold electrodes made from recordable CDs, Talanta 69 (2006) 877–881.
[21] J. Wang, B. Tiant, Mercury-free disposable lead sensors based on potentiometric stripping analysis at gold-coated screen-printed electrodes, Analytical Chemistry 65 (1993) 1529–1532.

Biographies

Robert D. Gardner obtained his BS and MS degrees in Biological Engineering at the Department of Biological and Irrigation Engineering, Utah State University in 2006 and 2008, respectively. He is currently pursuing his PhD degree in Chemical Engineering at Montana State University. His research interests include trace level chemical sensing and alternative energy development.

Nephi A. Zufelt received his BS degree in Mechanical Engineering from the Department of Mechanical and Aerospace Engineering, Utah State University 2006, and MS degree in Biomedical Engineering from the Joint Biomedical Engineering and

Imaging Department, The University of Tennessee and The University of Memphis 2008. His research focused on spine biomechanics and the effects of implanting spinal devices on the human spine. Nephi recently accepted a position as a Product Development Engineer with Choice Spine in Knoxville, Tennessee

Anhong Zhou is an assistant professor in the Department of Biological and Irrigation Engineering, Utah State University. He received his PhD degree in (Bio) analytical Chemistry from Hunan University, China, in 2000. His research interests include the development of biosensors for environmental quality monitoring and biomedical applications, biocorrosion, biological redox, and AFM applications in detecting cellular mechanics. Dr. Zhou is the member of American Chemical Society, Materials Research Society, Electrochemical Society, American Society for Engineering Education, and Institute of Biological Engineering.